Ionics (2021) 27:3251–3257
https://doi.org/10.1007/s11581-021-04102-0

ORIGINAL PAPER

Preparation and electrochemical performance of Na^+ and Co^{2+} co-doped $Li_{0.9}Na_{0.1}Mn_{1-x}Co_xPO_4$/C cathode material for Li-ion battery

Jun Zhang[1] · Shao-Hua Luo[2] · Qun-Xiang Ren[1] · Li-Li Sui[1] · Yan Qin[1] · Shu-Yan Zhang[3]

Received: 26 March 2021 / Revised: 3 May 2021 / Accepted: 14 May 2021 / Published online: 25 May 2021

Abstract

In this work, we have successfully in-situ synthesized Na^+ and Co^{2+} co-doped $Li_{0.9}Na_{0.1}Mn_{1-x}Co_xPO_4$/C nanoparticles on the surface of $Li_{2.7}Na_{0.3}PO_4$ self-sacrificing template by the co-precipitation process combined with the hydrothermal method. The crystal lattice structure, crystal appearance and electrochemical parameters are characterized by X-ray diffractometer (XRD), scanning electron microscopy (SEM), galvanostatic charge and discharge test, cyclic voltammetry (CV) and electrochemical impedance spectroscopy (EIS). SEM analysis indicates that $Li_{0.9}Na_{0.1}Mn_{0.9}Co_{0.1}PO_4$/C composite shows uniform porous structure and nanosized grain particles. The electrochemical measurements show that the double ions co-doping routine plays a vital influence on the rate capability and electrochemical lithium storage property of $LiMnPO_4$ material. The initial discharge specific capacity of $Li_{0.9}Na_{0.1}Mn_{0.9}Co_{0.1}PO_4$/C reaches 164.3 mAh/g (0.05 C) and 148.0 mAh/g (1 C), respectively. The excellent rate capability is attributed to the synergetic doping effect of Na^+ and Co^{2+} on improving the Li-ion diffusion rate and broadening the Li-ion diffusion channels.

Keywords Lithium ion battery · $LiMnPO_4$ · Na^+ and Co^{2+} co-doping effect · Electrochemical performance

Introduction

As new energy vehicles and electrochemical energy storage devices develop dramatically, the growing demands have been proposed on developing high energy/power densities lithium-ion power battery to satisfy people's production and living needs [1–5]. The cathode material is a critical ingredient of lithium-ion battery (LIBs); among the olivine phosphate family, $LiMnPO_4$ has been regarded as a significant cathode over commercial $LiFePO_4$ due to the superiority of discharge voltage platform, specific energy density (700 Wh/kg), superior safety and low price [6–9], which could also match the existing electrolytic liquid system. However, the high Li-ion diffusion activation energy and the one-dimensional channel lead to sluggish electronic/ionic conductivity and inferior electrochemical performance of $LiMnPO_4$ [10, 11]. The crystal structure transformation between $LiMnPO_4$/$MnPO_4$ caused by the Jahn-Teller effect would induce the collapse of lattice structure and the inferior cycle performance. To date, a good deal of modification methods [12–26] have been adopted to ameliorate electrochemical lithium storage property of $LiMnPO_4$/C. In general, the cation doping of $LiMnPO_4$ cathode with similar ionic radius to Mn^{2+} is an effective means to break through the barrier, the strategy of mutual cations doping at Li/Mn site could widen the one-dimensional Li-ion diffusion path, maintain the crystal structure stability and accelerate the Li-ion diffusion velocity [27, 28]. The selection of dopant is also a critical factor, the Co^{2+} (0.74 Å) has the similar ion radius to Mn^{2+} (0.80 Å), which is the main factor for choosing Co^{2+} as a dopant to inhibit lattice volume expansion and ameliorate the Jahn-Teller distortion of Mn^{3+} [29, 30]. Wang et al. [31] has synthesized the gradient Co-doped $LiMn_{0.98}Co_{0.02}PO_4$ by the secondary solvothermal method, the capacity retention of $LiMn_{0.98}Co_{0.02}PO_4$ is remarkably improved with the percentage of 87% after 380 cycles, the improvement is mainly due to the preferential growth along [010]-oriented $LiMnPO_4$ with more Li^+ migration channels and reaction sites. The Na-doped $Li_{0.9}Na_{0.1}MnPO_4$/C material

✉ Jun Zhang
junjun376@163.com

[1] College of Pharmacy, Shenyang Medical College, Shenyang 110034, People's Republic of China

[2] School of Resources and Materials, Northeastern University at Qinhuangdao, Qinhuangdao 066004, People's Republic of China

[3] Centre of Excellence for Advanced Materials, Dongguan 523808, People's Republic of China

[32] and the Na^+ and Ni^{2+} co-doped $Li_{0.9}Na_{0.1}Mn_{1-x}Ni_xPO_4/C$ cathode materials [23] have been studied in my research group, which show excellent discharge capacity and cycle stability. With the deepening of research, various methods have emerged to prepare double ions co-doped polyanionic-based $LiMnPO_4/C$ cathode materials [33–38]. Huang et al. [33] have prepared Fe^{2+} and Ti^{4+} co-doped $LiMnPO_4/C$ cathodes by a solid-state reaction route, the synergistic effect greatly enhances the electrochemical performance. Ramar and Balaya [34] have adopted a ball mill-assisted soft template method to synthesize the isovalent co-doped $LiMn_{0.9}Fe_{0.05}Mg_{0.05}PO_4/C$ sample, which shows higher lithium storage capacity (159 mAh/g, 0.1 C) and better cycling stability compared to $LiMnPO_4$ doped with either Fe^{2+} or Mg^{2+}. Recently, Li et al. [35] have adopted a solvothermal method to prepare $Li_{1-x}Na_xMn_{0.8}Fe_{0.2}PO_4/C$ nanocapsule; after 200 cycles, the capacity retention ratio is nearly 96.65% (0.5 C). Among these, hydrothermal approach has been selected as a high efficiency and good controllability synthesize method to optimize the electrochemical performances. Therefore, the strategy of cobalt ions and sodium ions co-doped at Mn/Li site seems to be a prospective attempt to enhance the electrochemical lithium storage performance of $LiMnPO_4$ through affording more lithium ions diffusion channels and reaction sites.

In this paper, we have adopted co-precipitation method to prepare $Li_{2.7}Na_{0.3}PO_4$ self-sacrificial template; subsequently, the nanosized $Li_{0.9}Na_{0.1}Mn_{1-x}Co_xPO_4/C$ cathode materials have been in-situ synthesized on the surface of $Li_{2.7}Na_{0.3}PO_4$ by a facile hydrothermal reaction. The microstructure, grains size and electrochemical characteristics of $Li_{0.9}Na_{0.1}Mn_{1-x}Co_xPO_4/C$ are systematically researched to evaluate the co-doping effect of Na^+ and Co^{2+} on improving the electrochemical properties of $LiMnPO_4/C$.

Experimental

Preparation

The different cobalt ion doping amounts of $Li_{0.9}Na_{0.1}Mn_{1-x}Co_xPO_4/C$ cathodes have in-situ synthesized through the hydrothermal method, using as-prepared $Li_{2.7}Na_{0.3}PO_4$ and $MnSO_4{\cdot}H_2O$ as mainly raw materials, $Co(NO_3)_2{\cdot}6H_2O$ as doping material. The $Li_{2.7}Na_{0.3}PO_4$ precursor has been successfully prepared in my previous work [32]. Other raw materials were analytically pure and commercially available without any treatment. To clarify the influence of cobalt ion doping on the electrochemical parameters of $Li_{0.9}Na_{0.1}Mn_{1-x}Co_xPO_4/C$ cathode materials, parallel experiments were conducted on maintaining all parameters that remain the same and only changing the contents of cobalt ions.

The synthesis process of $Li_{0.9}Na_{0.1}Mn_{1-x}Co_xPO_4/C$ was described as follows. Firstly, the $Li_{2.7}Na_{0.3}PO_4$, $MnSO_4{\cdot}H_2O$ and $Co(NO_3)_2{\cdot}6H_2O$ were, respectively, resolved in the PEG400-H_2O (V_{PEG400}/V_{H2O}=12 ml/24 ml) mixture solvents in a 1:1-x:x mole ratio, then the mixture solvents kept vigorous stirring for about 30 min to obtain the homogeneous solution. The above mixture solution was dissolved in a 50 ml Teflon-lined hydrothermal autoclave and reacted at 180 °C for 12 h. After the hydrothermal reaction, the synthetic substance was gathered after washing, centrifuged with deionized water and alcohol several times, then dryed in the oven at 80 °C for 8 h. Finally, the $Li_{0.9}Na_{0.1}Mn_{1-x}Co_xPO_4/C$ hydrothermal product was mixed and grinded with ascorbic acid in a mass fraction of 20 wt.% to form uniformly distributed ascorbic acid coated precursor; after calcination at 550 °C for 3 h in the flowing nitrogen gas atmosphere, the target $Li_{0.9}Na_{0.1}Mn_{1-x}Co_xPO_4/C$ were obtained.

The electrochemical properties of $Li_{0.9}Na_{0.1}Mn_{1-x}Co_xPO_4/C$ cathodes were measured by CR2032 coin cell, and fabricated in argon filled glove box. The cathode coating slurry was prepared through mixing the cathode material, PVDF binder and acetylene in a 8:1:1 mass ratio in NMP solvent under continuously vigorous stirring for 4 h. The aluminum foil collector was prepared by coating the cathode slurry on the aluminum foil, drying at 80 °C for 10 h in air, and the following 120 °C for 12 h under vacuum condition, aiming to evaporate the NMP and H_2O. After rolling and cutting, the 0.785 cm^2 circular sheet was formed. In the assembly process of CR2032 coin cells, lithium wafer, Celgard 2400 membrane and 1M $LiPF_6$/EC+MEC+DEC (volume ratio=1:1:1) mixture solution was served as the anode, separator and electrolyte in turn.

Characterization

The microstructures and crystal lattice data were tested by X-ray diffractometer (XRD, Rigaku Smartlab) with Cu Kα radiation under a sweep rate of 0.04°/s. The appearance of the crystal, grain size, pore structure of the doped materials were investigated by scanning electron microscopy (SEM, ZEISS SUPRA55) and transmission electron microscopy (TEM, JEOL JEM2100F). The concentration of Mn^{2+} and Co^{2+} resolved in the electrolyte was measured by the inductively coupled plasma-atomic emission spectrometer (ICP-AES, PS-6).

The electrochemical parameters of the CR2032 coin cell was measured by the charge/discharge measurements on the Land CT2001A battery tester within the wide operating voltage range (2.5–4.5 V). The charge transfer kinetics and electrode polarization phenomenon were tested by CV and EIS methods on the Solartron 1260+1287 electrochemical workstation. The EIS test frequency was in the range of 10^{-1}–10^5 Hz, and the voltage amplitude was set to 10 mV. The CV test

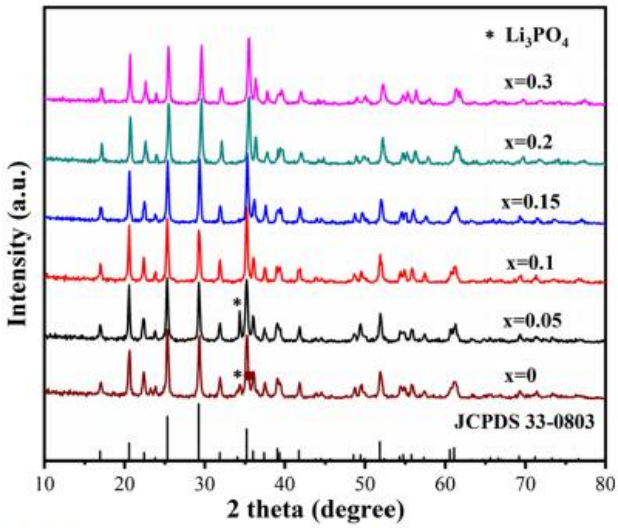

Fig. 1 XRD diffraction patterns of $Li_{0.9}Na_{0.1}Mn_{1-x}Co_xPO_4/C$ (x = 0, 0.05, 0.1, 0.15, 0.2, 0.3) samples

voltage range was on the scale of 2.5–4.5 V at a 0.1 mV/s sweep rate. All measurements were tested at ambient temperature.

Results and discussion

The Na^+ and Co^{2+} co-doped $Li_{0.9}Na_{0.1}Mn_{1-x}Co_xPO_4/C$ samples have been synthesized through the hydrothermal method; in the doped samples, the doping ratio of Na^+ is fixed at 0.1, and vary the Co^{2+} contents ratio (x) with 0, 0.05, 0.1, 0.15, 0.2, 0.3. Fig. 1 displays the XRD patterns of $Li_{0.9}Na_{0.1}Mn_{1-x}Co_xPO_4/C$ samples, and the JCPDS standard card of $LiMnPO_4$ (No. 33-0803). The main characteristic diffractive peaks of all doped samples are well indexed with the orthorhombic system (Pnmb) of $LiMnPO_4$. From the Riteveld lattice parameters of all the $Li_{1-x}Na_xMnPO_4/C$ diffraction patterns calculated by High Score Software, we have found that the lattice constant values of Co-doped samples change little with no obvious regularity, which is largely due to the similar ion radius of Co^{2+} (0.74 Å) to Mn^{2+} (0.80 Å). In the sample of x = 0 and x = 0.05, an additional diffraction peak is observed at 34.4°, which is associated with Li_3PO_4 phase (JCPDS card No. 25-1030), and in accordance with our previous research [32]. There are no evident impurities and carbon diffraction peaks, which means that the pyrolytic carbon exists in amorphous form. This indicates that Na^+ and Co^{2+} have embedded into the crystal lattice of $LiMnPO_4$, and a certain amount of Na^+ and Co^{2+} could not influence the crystal structure of the doped samples. The shape of the diffraction peaks is very narrow and strong mean the high crystallinity of the as-prepared materials.

Figure 2 displays the SEM photographs of different cobalt ion doping amounts of $Li_{0.9}Na_{0.1}Mn_{1-x}Co_xPO_4/C$ samples. It can be found that the morphologies of all samples present similar microstructures with irregular spherical-like shape primary particles aggregating together. The average diameters of the primary particles are ranging from 40 to 80 nm. When the cobalt doping ratio (x) is 0.1, the inner pore structure seems more uniform in distribution, indicating that an appropriate cobalt doping ratio could effectively increase the reactivity between active material and electrolytes across the two-phase interface. The real chemical compositions of $Li_{0.9}Na_{0.1}Mn_{0.9}Co_{0.1}PO_4/C$ sample are measured by ICP, and the practical molar ratio of Li:Na:Mn:Co:P is 0.907:0.093:0.897:0.103:1.000. The results are nearly the designed stoichiometric ratio of 0.9:0.1:0.9:0.1:1.

Figure 3 shows the TEM photographs of $Li_{0.9}Na_{0.1}Mn_{0.9}Co_{0.1}PO_4/C$ sample. Numerous nanosized grains stack tightly together with the average diameters of

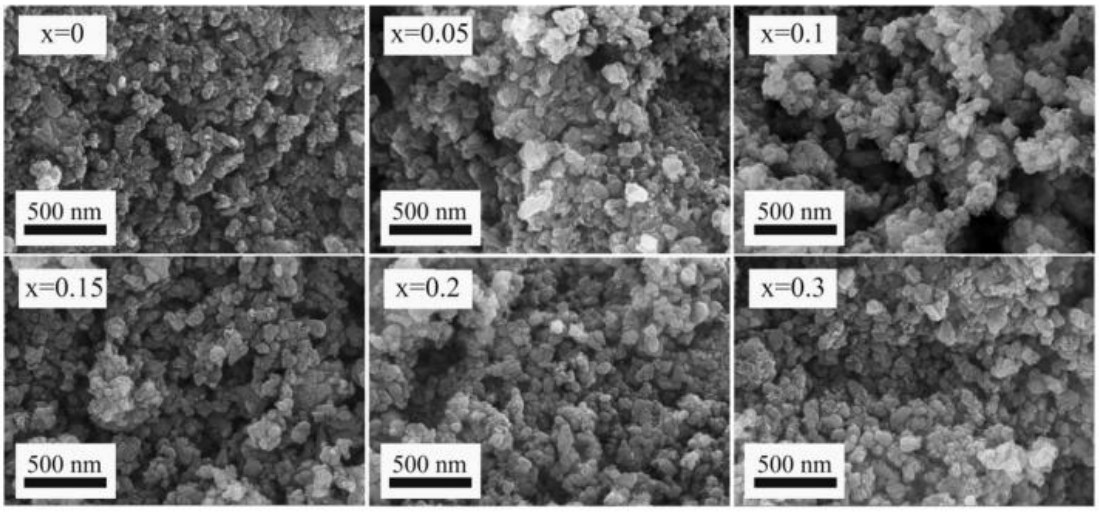

Fig. 2 SEM photographs of as-prepared $Li_{0.9}Na_{0.1}Mn_{1-x}Co_xPO_4/C$(x = 0, 0.05, 0.1, 0.15, 0.2, 0.3) samples

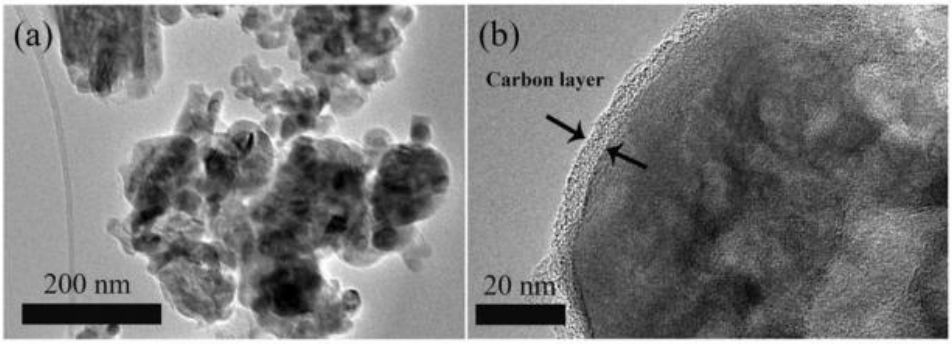

Fig. 3 TEM photographs of $Li_{0.9}Na_{0.1}Mn_{0.9}Co_{0.1}PO_4$/C sample

22–58 nm. It can be seen from the high-magnification TEM photograph in Fig. 3(b), the continuous carbon layer is uniformly coated on the surface of the nanoparticles with the thickness of 4–5 nm, which is obtained by the pyrolysis of carbon sources. The uniform conductive carbon layer will facilitate the electronic transfer in the surface layer of the cathode materials.

The galvanostatic charge/discharge measurements of different Co^{2+} doping amounts of $Li_{0.9}Na_{0.1}Mn_{1-x}Co_xPO_4$/C samples are tested at 0.05 C discharge rate, the charging and discharging curves are displayed in Fig. 4. All the discharging curves exhibit a lank voltage platform nearly 4.05 V (vs. Li/Li^+), which are attributed to redox reaction between the redox couple of Mn^{3+}/Mn^{2+}. The doping amounts of Co^{2+} greatly affect influence the discharge specific capacity of $Li_{0.9}Na_{0.1}MnPO_4$/C. As the Co^{2+} doping amounts increase, the initial discharge capacity are 152.0 mAh/g, 153.5 mAh/g, 164.3 mAh/g, 144.6 mAh/g, 137.4 mAh/g and 128.2 mAh/g, respectively. For all samples, $Li_{0.9}Na_{0.1}Mn_{0.9}Co_{0.1}PO_4$/C delivers relatively high discharge capacity. The capacity enhancement is attributed to a moderate cobalt ion doping amount that could effectively improve intrinsic conductivity and increase reactive sites during the Li-ion insertion/deinsertion process. However, excessive Co^{2+} doping contents would cause capacity deterioration. The cycle stability and rate performance are tested to reflect the electrochemical performance of the doped samples. The cycle performance of $Li_{0.9}Na_{0.1}Mn_{1-x}Co_xPO_4$/C composites is measured at 0.05 C, and the cyclic curves are shown in Fig. 5(a). After 200 cycles, $Li_{0.9}Na_{0.1}Mn_{0.9}Co_{0.1}PO_4$/C and $Li_{0.9}Na_{0.1}MnPO_4$/C decrease to the similar discharge capacity value, but still higher than other cobalt ion doping samples. The conclusions indicate that excessive Co^{2+} doping amounts would lead to poor cycle performance. Fig. 5(b) shows the rate capability of the doped samples measured at different rates. Obviously, $Li_{0.9}Na_{0.1}Mn_{0.9}Co_{0.1}PO_4$/C electrode shows excellent rate discharge performance, and in different rate, the discharge capacity is 164.3 mAh/g (0.05 C), 160.4 mAh/g (0.1 C), 155.3 mAh/g (0.2 C), 152.9 mAh/g (0.5 C) and 148.0 mAh/g (1 C), respectively. The discharge capacity slightly decreases with the discharge rate increasing. It indicates that a proper amount of Co^{2+} doping is beneficial to obtain high rate performance of the cathode material by means of maintaining the structural stability and broadening the lithium ions diffusion channel during the Li-ion insertion/deinsertion process.

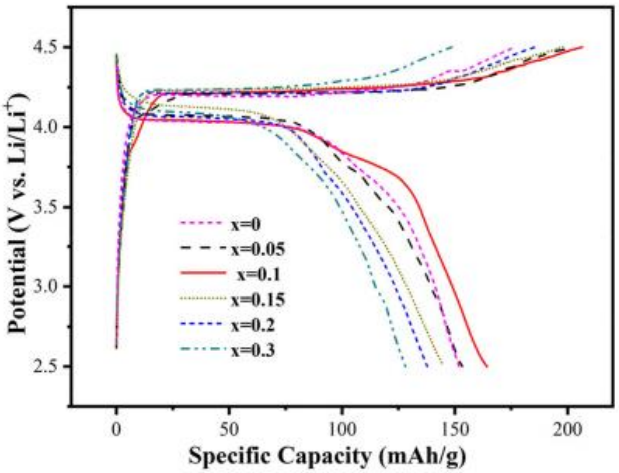

Fig. 4 The first charge/discharge curves of $Li_{0.9}Na_{0.1}Mn_{1-x}Co_xPO_4$/C(x = 0, 0.05, 0.1, 0.15, 0.2, 0.3) samples at 0.05 C

The EIS test has been conducted to analyze the reaction kinetics on the interface of two-phase media of $Li_{0.9}Na_{0.1}Mn_{1-x}Co_xPO_4$/C composite materials. Fig. 6(a) shows the EIS curves of all the doped samples, the Nyquist curves are composing of a semicircular shape and an oblique line two parts, respectively located in the high-middle frequency range and the low frequency range. The intercept of the semicircular on the axis of reals is corresponding to the complex charge transfer resistance (R_{ct}). The slope of the straight line represents the lithium ion diffusion velocity (W_o). The value of R_{ct} is different. The $Li_{0.9}Na_{0.1}Mn_{0.9}Co_{0.1}PO_4$/C sample exhibits the smallest R_{ct} value, indicating that $Li_{0.9}Na_{0.1}Mn_{0.9}Co_{0.1}PO_4$/C shows the smallest charge transfer resistance. For further understanding the Na^+ and Co^{2+} co-doping effects on the charge transfer dynamics, we have fitted the EIS results and the linear fitting curves between Z' and $w^{-1/2}$ are represented inset in Fig. 6(a). According to the equation $Z' = R_s + R_{ct} + \sigma w^{-1/2}$, we could obtain the Warburg factor (σ) of all the samples by calculating the slope of the equation. The

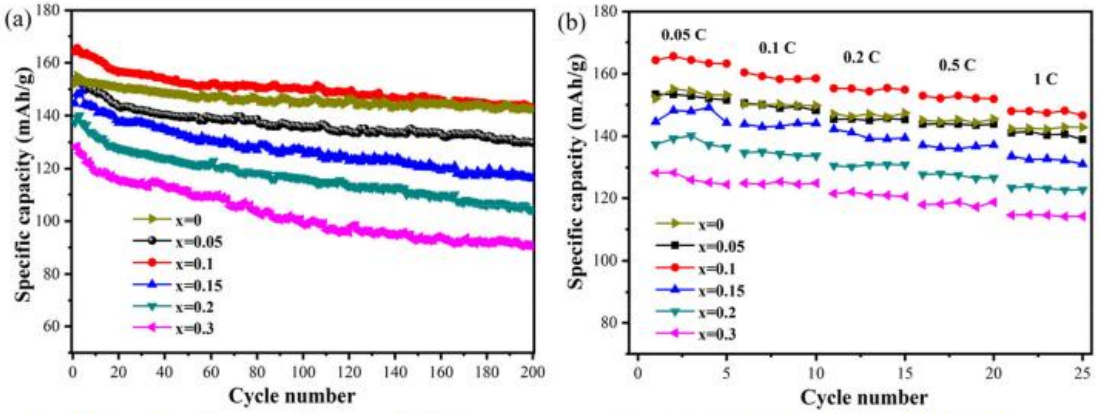

Fig. 5 The cycling ability (**a**) and the rate performance (**b**) of $Li_{0.9}Na_{0.1}Mn_{1-x}Co_xPO_4/C$ (x = 0, 0.05, 0.1, 0.15, 0.2, 0.3) samples

$Li_{0.9}Na_{0.1}Mn_{0.9}Co_{0.1}PO_4/C$ shows the lower σ value, which means that the sample has the higher lithium ion diffusion coefficient (D_{Li^+}). The results show that $Li_{0.9}Na_{0.1}Mn_{0.9}Co_{0.1}PO_4/C$ has low electrode polarization and excellent reaction kinetics in the Li-ion insertion/deinsertion process. In a word, the synergistic effects of Na^+ and Co^{2+} co-doped are beneficial to Li-ion diffusion in the lattice structure of the cathode materials.

From the CV plots of $Li_{0.9}Na_{0.1}MnPO_4/C$ and $Li_{0.9}Na_{0.1}Mn_{0.9}Co_{0.1}PO_4/C$ samples in Fig. 6(b), a couple of good symmetrical reversible redox peaks have been found, which are assigned to the redox reaction of Mn^{3+}/Mn^{2+} accompanied with the Li-ion insertion/deinsertion process. The redox process is a quasi-reversible reaction. In the cycle process, the redox voltage difference values of $Li_{0.9}Na_{0.1}MnPO_4/C$ and $Li_{0.9}Na_{0.1}Mn_{0.9}Co_{0.1}PO_4/C$ are close to 0.54 and 0.43 V. With the adding of cobalt ions, the potential interval decreases slightly with no serious electrode polarization, illustrating that a proper doping ratio of Na^+ and Co^{2+} is favorable to improve the reaction reversibility and reduce electrode polarization rate of $LiMnPO_4/C$.

Conclusions

In this work, Na^+ and Co^{2+} co-doped $Li_{0.9}Na_{0.1}Mn_{1-x}Co_xPO_4/C$ nanoparticles have been successfully in-situ prepared on the surface of $Li_{2.7}Na_{0.3}PO_4$ self-sacrificing template through the co-precipitation process combined with the hydrothermal method. A proper doping ratio of Co^{2+}/Na^+ is beneficial to reduce the grain size, increase pore size and porosity, and further improve the migration velocity of lithium ion. By comparing with other doped samples, $Li_{0.9}Na_{0.1}Mn_{0.9}Co_{0.1}PO_4/C$ sample shows the superior high discharge capacity of 164.3 mAh/g (0.05 C) and 148.0 mAh/g (1 C), which exhibit excellent discharge performance induced by the abundant pore structure and the widened Li-ion diffusion channel of the cathode material.

Acknowledgements The work was funded by the National Natural Science Fund of China (Nos. 51874079, 51674068), Liaoning Province Ordinary Higher Education Institutions Intercollegiate Cooperation Project (No. 202010), Liaoning Province Education Department Science and Technology Research Project (No. 202006), Scientific

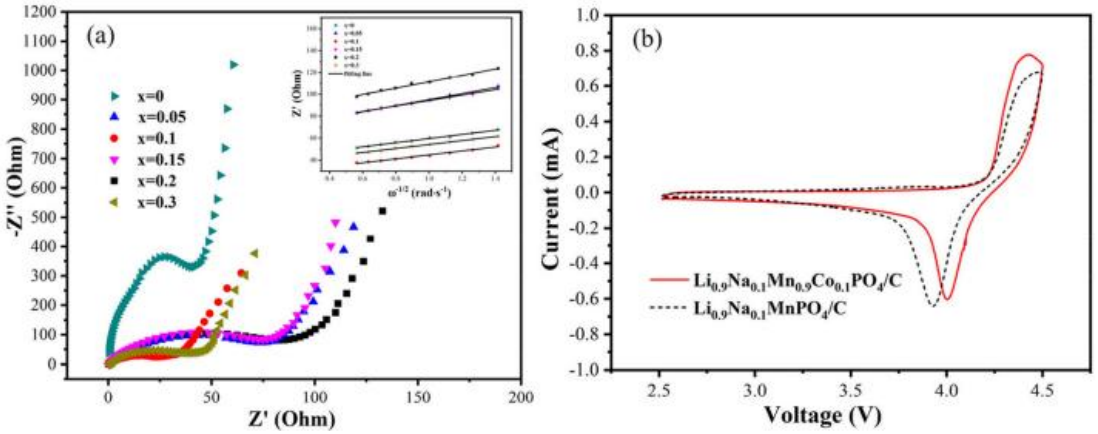

Fig. 6 (**a**) The EIS curves of $Li_{0.9}Na_{0.1}Mn_{1-x}Co_xPO_4/C$(x = 0, 0.05, 0.1, 0.15, 0.2, 0.3) samples, inset: the linear fitting curves; (**b**) The CV plots of $Li_{0.9}Na_{0.1}MnPO_4/C$ and $Li_{0.9}Na_{0.1}Mn_{0.9}Co_{0.1}PO_4/C$ samples

Research Fund of Shenyang Medical College (No. 20201006), Science and Technology Fund of Shenyang Medical College (No. 20195076), Supported by the Program for Guangdong Introducing Innovative and Entrepreneurial Teams (No. 2016ZT06G025).

References

1. Wan Y, Zheng QJ, Lin DM (2014) Recent development of $LiMnPO_4$ as cathode materials of lithium-ion batteries. Acta Chim Sin 72:537–551
2. Luo SH, Tang ZL, Lu JB, Zhang ZT (2008) Electrochemical properties of carbon-mixed $LiFePO_4$ cathode material synthesized by the ceramic granulation method. Ceram Int 34:1349–1351
3. Martha SK, Markovsky B, Grinblat J (2009) $LiMnPO_4$ as an advanced cathode material for rechargeable lithium batteries. J Electrochem Soc 156:A541–A552
4. Luo SH, Hu D, Liu H, Li J, Yi TF (2019) Hydrothermal synthesis and characterization of α-Fe_2O_3/C using acid pickled iron oxide red for Li-ion batteries. J Hazard Mater 368:714–721
5. Bao S, Luo S, Yan S, Wang Z, Wang Q, Feng J, Wang Y, Yi T (2019) Nano-sized MoO_2 spheres interspersed three-dimensional porous carbon composite as advanced anode for reversible sodium/potassium ion storage. Electrochim Acta 307:293–301
6. Bao L, Chen Y, Xu G, Yang T (2018) Hydrothermal synthesis of monodispersed $LiMnPO_4$ (010) nanobelts and [001] nanorods and their applications in lithium-ion batteries. Eur J Inorg Chem (13): 1533–1539
7. Hu XD, Sun XH, Yang M, Ji HM, Li XL, Cai S, Guo RS et al (2016) Sandwich nanostructured $LiMnPO_4$/C as enhanced cathode materials for lithium-ion batteries. J Mater Sci 52(7):3597–3612
8. Long YF, Su J, Cui XR, Lv XY, Wen YX (2015) Enhanced rate performance of $LiFePO_4$/C by co-doping titanium and vanadium. Solid State Sci 48:104–111
9. Li JZ, Luo SH, Wang Q et al (2018) Facile synthesis of carbon-$LiMnPO_4$ nanorods with hierarchical architecture as a cathode for high-performance Li-ion batteries. Electrochim Acta 289:415–421
10. Bezza I, Kaus M, Heinzmann R (2015) Mechanism of the delithiation/lithiation process in $LiFe_{0.4}Mn_{0.6}PO_4$: in situ and ex situ investigations on long-range and local structures. J Phys Chem C 119:9016–9024
11. Esmezjan L, Mikhailova D, Etter M, Cabana J, Grey CP, Indris S, Ehrenberg H (2019) Electrochemical lithium extraction and insertion process of sol-gel synthesized $LiMnPO_4$ via two-phase mechanism. J Electrochem Soc 166(6):A1257–A1265
12. Xie Z, Chang K, Li B, Tang H, Fu X, Chang Z, Yuan XZ, Wang H (2016) Glucose-assisted synthesis of highly dispersed $LiMnPO_4$ nanoparticles at a low temperature for lithium ion batteries. Electrochim Acta 189:205–214
13. Ragupathi V, Panigrahi P, Nagarajan GS (2019) Enhanced electrochemical performance of nanopyramid-like $LiMnPO_4$/C cathode for lithium-ion batteries. Appl Surf Sci 495:143541
14. Pan X, Gao Z, Liu L, Xiao F, Xiao F, Xie S, Yi R (2019) Self-templating preparation and electrochemical performance of $LiMnPO_4$ hollow microspheres. J Alloys Compd 783:468–477
15. Kwon NH, Yin H, Vavrova T, Lim JHW, Steiner U, Grobéty B, Fromm KM (2017) Nanoparticle shapes of $LiMnPO_4$, Li^+ diffusion orientation and diffusion coefficients for high volumetric energy Li^+ ion cathode. J Power Sources 342:231–240
16. Wang L, Zhang H, Liu Q, Wang J, Ren Y, Zhang X, Yin G (2018) Modifying high-voltage olivine-type $LiMnPO_4$ cathode via Mg substitution in high-orientation crystal. ACS Appl Energy Mater 1(11):5928–5935
17. Gutierrez A, Qiao R, Wang L (2014) High-capacity, aliovalently doped olivine $LiMn_{1-3x/2}V_{x\square x/2}PO_4$ cathodes without carbon coating. Chem Mater 26(9):3018–3026
18. Vasquez FA, Calderon JA (2019) Vanadium doping of $LiMnPO_4$ cathode material: correlation between changes in the material lattice and the enhancement of the electrochemcial performance. Electrochim Acta 325:134930
19. Khalfaouy RE, Addaou A, Laajeb A (2019) Synthesis and characterization of Na-substituted $LiMnPO_4$ as a cathode material for improved lithium ion batteries. J Alloys Compd 775:836–844
20. Zhu YR, Zhang R, Deng L, Yi TF (2015) Lithium-ion insertion kinetics of Na-doped $LiFePO_4$ as cathode materials for lithium-ion batteries. Metall Mater Trans E 2(1):33–38
21. Rajammal K, Sivakumar D (2017) Na-doped $LiMnPO_4$ as an electrode material for enhanced lithium ion batteries. Bull Mater Sci 40(1):171–175
22. Chen W, Fang H (2019) Communication-aluminum doping in $LiMnPO_4$ with an unexpected charge compensation. J Electrochem Soc 166(13):A2752–A2754
23. Zhang J, Luo SH, Sui LL, Sun YY (2018) Co-precipitation assisted hydrothermal method to synthesize $Li_{0.9}Na_{0.1}Mn_{0.9}Ni_{0.1}PO_4$/C nanocomposite as cathode for lithium ion battery. J Alloys Compd 768:991–994
24. Zhang J, Luo S, Wang Q (2017) Yttrium doping at Mn-site to improve electrochemical kinetics activity of sol-gel synthesized $LiMnPO_4$/C as cathode for lithium ion battery. J Solid State Electrochem 21(11):3189–3194
25. Zhang J, Luo S, Chang L (2016) In-situ growth of $LiMnPO_4$ on porous $LiAlO_2$ nanoplates substrates from AAO synthesized by hydrothermal reaction with improved electrochemical performance. Electrochim Acta 193:16–23
26. Dinh HC, Mho S, Kang Y (2013) Large discharge capacities at high current rates for carbon-coated $LiMnPO_4$ nanocrystalline cathodes. J Power Sources 244:189–195
27. Ouyang C, Shi S, Wang Z (2004) First-principles study of Li ion diffusion in $LiFePO_4$. Phys Rev B 69(10):104303
28. Morgan D, Van der Ven A, Ceder G (2004) Li conductivity in $LixMPO_4$ (M= Mn, Fe, Co, Ni) olivine materials. Electrochem Solid-State Lett 7(2):A30–A32
29. Yang G, Ni H, Liu H, Gao P, Ji H, Roy S (2011) The doping effect on the crystal structure and electrochemical properties of $LiMn_xM_{1-x}PO_4$(M=Mg, V, Fe, Co, Gd). J Power Sources 196(10):4747–4755
30. Ma F, Zhang X, He P, Zhang X, Wang P, Zhou H (2011) Synthesis of hierarchical and bridging carbon-coated $LiMn_{0.9}Fe_{0.1}PO_4$ nanostructure as cathode material with improved performance for lithium ion battery. J Power Sources 359(15):408–414
31. Wang RJ, Zheng JY, Feng XM, Ge Y (2020) Highly [010]-oriented, gradient Co-doped $LiMnPO_4$ with enhanced cycling stability as cathode for Li-ion batteries. J Solid State Electrochem 24: 511–519
32. Zhang J, Luo SH, Ren QX, Zhang DJ, Qin Y (2020) Tailoring the sodium doped $LiMnPO_4$/C orthophosphate to nanoscale as a high-performance cathode for lithium ion battery. Appl Surf Sci 530: 146628
33. Huang QY, Wu Z, Su J, Long YF, Lv XY, Wen YX (2016) Synthesis and electrochemical performance of Ti–Fe co-doped $LiMnPO_4$/C as cathode material for lithium-ion batteries. Ceram Int 42:11348–11354
34. Ramar V, Balaya P (2013) Enhancing the electrochemical kinetics of high voltage olivine $LiMnPO_4$ by isovalent co-doping. Phys Chem Chem Phys 15:17240–17249
35. Li R, Fan CL, Zhang WH, Tan MC (2019) Structure and performance of Na^+ and Fe^{2+} co-doped $Li_{1-x}Na_xMn_{0.8}Fe_{0.2}PO_4$/C nanocapsule synthesized by a simple solvothermal method for lithium ion batteries. Ceram Int 45:10501–10510

36. Lv XY, Cui XR, Long YF, Su J, Wen YX (2015) Optimization of titanium and vanadium co-doping in $LiFePO_4$/C using response surface methodology. Ionics 21(9):2447–2455
37. Su J, Liu ZZ, Long YF, Yao H, Lv XY, Wen YX (2015) Enhanced electrochemical performance of $LiMnPO_4$/C prepared by microwave-assisted solvothermal method. Electrochim Acta 173: 559–565
38. Sronsri C, Noisong P, Danvirutai C (2016) Synthesis, characterization and vibrational spectroscopic study of Co, Mg co-doped $LiMnPO_4$. Spectrochim Acta A 153:436–444